

Morphologic analysis with computed tomography may help differentiate fat-poor angiomyolipoma from renal cell carcinoma: a retrospective study with 602 patients

Yong Hee Kim,¹ Kyunghwa Han,¹ Young Taik Oh,¹ Dae Chul Jung,¹ Nam Hoon Cho,² Sung Yoon Park¹

¹Department of Radiology, Yonsei University College of Medicine, 50 Yonsei-ro, Seodaemun-gu, Seoul 120-752, Republic of Korea

²Department of Pathology, Yonsei University College of Medicine, Seoul, Republic of Korea

Abstract

Purpose: To assess whether morphologic analysis using computed tomography (CT) could differentiate between fat-poor angiomyolipoma (fpAML) and renal cell carcinoma (RCC).

Methods: A total of 602 patients with a histologically confirmed fpAML ($n = 49$) or RCC ($n = 553$) were evaluated. All renal lesions were less than 4 cm in size and had no gross fat on contrast-enhanced CT. For morphologic analysis, overflowing beer sign and angular interface were evaluated. Overflowing beer sign was defined as contact length between bulging-out portion of a mass and the adjacent renal capsule of 3 mm or greater. Angular interface was defined as the angle of parenchymal portion of a mass of 90° or less. Sensitivity, specificity, positive predictive value (PPV), negative predictive value (NPV), and accuracy were assessed. Multivariate analysis was conducted to determine which variable is predictive of fpAML.

Results: Sensitivity, specificity, PPV, NPV, and accuracy were 61.2% (30/49), 97.1% (537/553), 65.2% (30/46), 96.6% (537/556), and 94.2% (567/602) with overflowing beer sign, while they were 55.1% (27/49), 81.9% (453/553), 21.3% (27/127), 95.4% (453/475), and 79.7% (480/602) with angular interface for fpAML, respectively. Both CT variables were predictive of fpAML (overflowing beer sign, odds ratio = 132.881, $p < 0.001$; angular interface, odds ratio = 5.766, $p = 0.010$). The multivariate model with CT variables showed good performance for predicting fpAML (AUC, 0.871 with angular

interface, 0.943 with overflowing beer sign, and 0.949 with both).

Conclusion: Morphologic analysis with contrast-enhanced CT may be useful for differentiating fpAML from RCC. Overflowing beer sign has the potential as an imaging biomarker for fpAML.

Key words: Angiomyolipoma—Renal cell carcinoma—Fat-poor—Computed tomography—Overflowing beer sign

Interpretation of imaging features alone is limited in reliable differentiation between fat-poor angiomyolipoma (fpAML) and renal cell carcinoma (RCC) [1, 2]. Accordingly, 4%–13% of small (≤ 4 cm) renal masses were proven as AML after pathologic examination [3–6]. Thus, histologic confirmation with the percutaneous biopsy sometimes provides useful information for patients who are the candidates of active surveillance or focal ablative therapies [1, 7, 8]. However, percutaneous biopsy is invasive, and sometimes unavailable or less effective for uncooperative patients, patients with uncorrectable coagulopathy, or those with very small renal lesions [9–11]. Therefore, identifying radiologic clues suggestive of fpAML can non-invasively help plan management strategy.

Computed tomography (CT) has been widely used for a long time to evaluate renal masses and is relatively less expensive than magnetic resonance imaging (MRI) [1]. Many studies have reported that quantitative analyses of CT data may be helpful in diagnosing fpAML [12–14]. Nevertheless, there are still some overlaps in quantitative

imaging features. In addition, different CT regimens in image acquisition between the institutions may hamper the widespread use of quantitative data with a uniform standard [15, 16].

Meanwhile, morphologic features may be easily recognized across various imaging protocols. Researchers have reported that morphologic analysis of the renal mass using CT or MRI can help differentiate between RCC and benign lesions including AML [17–19]. In the studies, radiologic findings of non-round shape, or angular interface which means narrow, angular configuration of parenchymal portions of a tumor, were significant predictors of benign renal masses or fpAML.

Recently, we noticed that the bulging-out portions of some small fpAML extend along the adjacent renal surface on contrast-enhanced CT, a finding we termed ‘overflowing beer sign.’ In this study, we investigated whether or not morphologic analysis of the angular interface or overflowing beer sign on contrast-enhanced CT is useful for the differentiation between fpAML and RCC.

Methods

Patients

This study was approved by the Institutional Review Board, and the requirement for informed consent was waived. Between January 2006 and May 2015, a total of 1233 patients with contrast-enhanced CT and histologically proven RCC or AML less than 4 cm in size were found through chart review (Fig. 1). Among them, 631 patients were excluded as follows: (a) section thickness of CT greater than 3 mm ($n = 490$), (b) cystic mass ($n = 72$), (c) intralesional gross fat ($n = 52$), (d) lesion

size less than 1 cm ($n = 9$), (e) multiple renal lesions ($n = 7$), and (f) severe motion artifact ($n = 1$). We excluded patients with section images greater than 3 mm to minimize possible partial volume artifact mimicking overflowing beer sign [20]. The proportion of AML ($p = 0.799$) or sex ($p = 0.622$) was similar between the final study group and the excluded group due to the section thickness. The patients with cystic mass or intralesional gross fat on CT images were excluded because those are well-established imaging features predicting AML or not [21, 22], so that the analysis of angular interface or overflowing beer sign may not provide added value for the differentiation. Thus, a total of 602 patients (mean age, 55.8 ± 12.6 years) with RCC ($n = 553$) or fpAML ($n = 49$) were finally included in this study. The patient characteristics are summarized in Table 1.

CT examination

CT examination was performed with one of eight multi-detector scanners (Sensation 64, Somatom Definition AS+, or Somatom Definition Flash, Siemens, Germany; Light-speed VCT or Discovery CT 750 HD, GE, USA; iCT 128 or Ingenuity CT, Philips, Netherlands; or Aquilion, Toshiba, Japan). The contrast-enhanced ima-

Table 1. Characteristics of the patients

Parameter	RCC ($n = 533$)	fpAML ($n = 49$)	p value
Age (years)	56.1 ± 12.5	51.6 ± 12.8	0.014
Gender (M : F)	374 : 179 (67.6% : 32.4%)	9 : 40 (18.4% : 81.6%)	<0.001
Size (mm)	22.4 ± 7.8	17.9 ± 7.1	<0.001

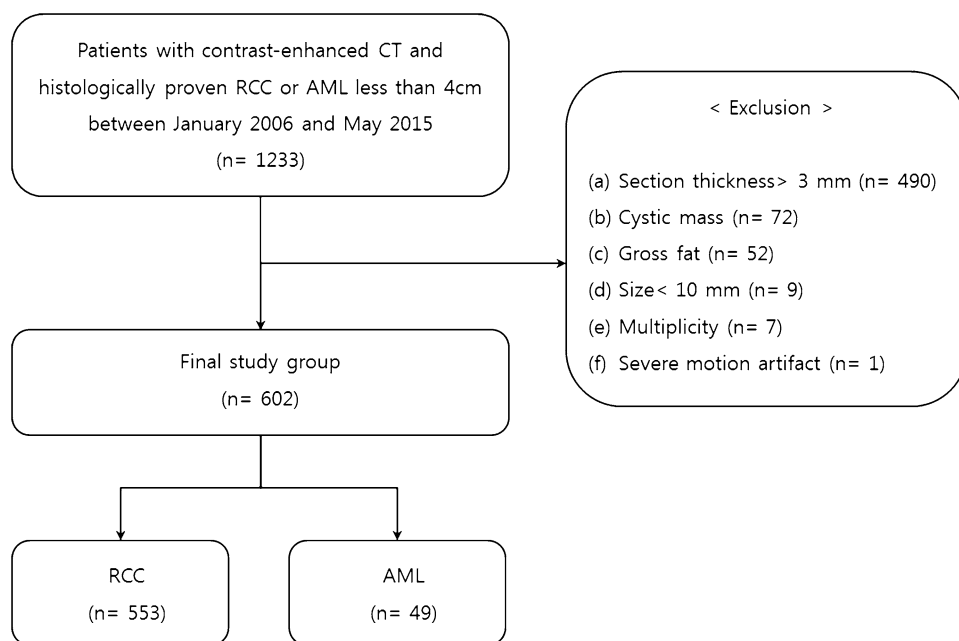


Fig. 1. Flowchart of study patients.

ges were obtained using the non-ionic contrast agents (Xenetix 300, Guerbet, France; Iopamiro 370, Bracco, Italy; Ultravist 300 or 370, Bayer Schering Pharma, Germany; or Pamiray 370, Dongkook Pharma, Korea). The CT protocols were as follows: axial and coronal planes, 80–120 kVp, variable tube current, and a section thickness of 3 mm. However, we could not uniformly standardize the other CT protocols such as the image acquisition time because a substantial number of CT examinations were performed at outside hospitals. All images were archived using the PACS (PathSpeed Workstation, GE Healthcare) for analysis.

Image interpretation

Two radiologists (reader 1, S.Y.P., a faculty with 5 years of experience reading abdominal CT; reader 2, Y.H.K., a senior resident with experience reading more than 1000 abdominal CT cases) who were blinded to pathologic information analyzed CT images in consensus. For all patients, the size of a renal mass was measured on contrast-enhanced CT images.

For morphologic analysis, overflowing beer sign and angular interface were evaluated on axial and coronal planes, respectively. When the most prominent findings were observed in either plane, it was considered to be representative of a particular patient. The contact length between bulging-out portion of a mass and the adjacent renal surface was measured on contrast-enhanced CT images (Fig. 2). The angle of parenchymal portion of a mass was classified into three subgroups: (a) angle $<45^\circ$,

(b) $45^\circ \leq \text{angle} \leq 90^\circ$, and (c) angle $>90^\circ$. The angle $>90^\circ$ indicated the obtuse angle or round parenchymal interface.

The reference standard was the pathologic report of medical record, the results of which were finally reviewed and confirmed by an experienced genitourinary pathologist (N.H.C.).

Statistical analysis

Statistical analyses were performed using SAS (version 9.4, SAS Institute Inc., Cary, NC, USA). A p value of less than 0.05 was considered statistically significant.

The Chi-square test was utilized to compare the patient age or gender and lesion size between RCC and fpAML, and the proportion of angle subgroups between RCC and fpAML. The independent t test was conducted to compare the contact length suggestive of overflowing beer sign between RCC and fpAML. ROC curve analysis was performed to assess the area under the curve (AUC) and optimal cutoff of overflowing beer sign and angular interface for diagnosing fpAML.

We compared the sensitivity, specificity, positive predictive value (PPV), negative predictive value (NPV), and accuracy of the overflowing beer sign and angular interface for the diagnosis of fpAML using the logistic regression with generalized estimating equation. In addition, the estimated PPV and NPV were calculated based on Bayes' theorem using the prevalence of published studies [23].

Univariate and multivariate logistic regression analyses were also conducted to analyze whether morphologic findings of CT are predictive of fpAML. We designed four models as follows: (a) model 1 consisted of age, sex, and lesion size; (b) model 2 consisted of age, sex, lesion size, and angular interface; (c) model 3 consisted of age, sex, lesion size, and overflowing beer sign; and (d) model 4 included all the parameters. The Hosmer–Lemeshow test was performed to assess the goodness of fit of each model [24, 25]; in the Hosmer–Lemeshow test, $p > 0.05$ indicated that the calibration of the model is adequate. We also analyzed the AUCs of each prediction model to estimate the performance for fpAML [24, 25] and compared them using Delong test with post hoc Bonferroni correction for multiple comparisons.

Results

The mean age of the patients with RCC (56.1 ± 12.5 years) was higher than that of the patients with fpAML (51.6 ± 12.8 years) ($p = 0.014$). The female proportion was significantly higher in fpAML than RCC (fpAML, 81.6%; RCC, 32.4%; $p < 0.001$). The mean size of patients with RCC (22.4 ± 7.8 mm) was higher than that of those with fpAML (17.9 ± 7.1 mm) ($p < 0.001$).

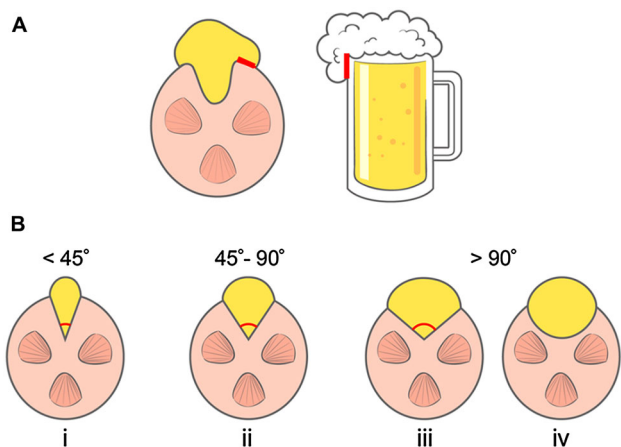


Fig. 2. Schematic illustrations of overflowing beer sign and angular interface. **A** The contact length ≥ 3 mm of bulging-out portion of a renal tumor onto the renal surface indicated positive overflowing beer sign (red line). **B** The angle of parenchymal portion of a mass was classified into three subgroups (angle $<45^\circ$, $45^\circ \leq \text{angle} \leq 90^\circ$, angle $>90^\circ$). The angle $>90^\circ$ indicated the obtuse angle or round parenchymal interface (iii or iv). The angular interface was defined as the angle of 90° or less (i or ii).

Table 2. Comparison of diagnostic performance between overflowing beer sign and angular interface

Parameter	Overflowing beer sign	Angular interface	p value
Sensitivity	61.2 (30/49) [46.2–74.8]	55.1 (27/49) [40.2–69.3]	0.490
Specificity	97.1 (537/553) [95.3–98.3]	81.9 (453/553) [78.4–85.0]	<0.001
PPV	65.2 (30/46) [49.8–78.7]	21.3 (27/127) [14.5–29.4]	<0.001
NPV	96.6 (537/556) [94.7–97.9]	95.4 (453/475) [93.1–97.1]	0.139
Accuracy	94.2 (567/602) [92.0–95.9]	79.7 (480/602) [76.3–82.9]	<0.001

PPV positive predictive value, NPV negative predictive value
The data are % (number of patients) [95% confidence interval]

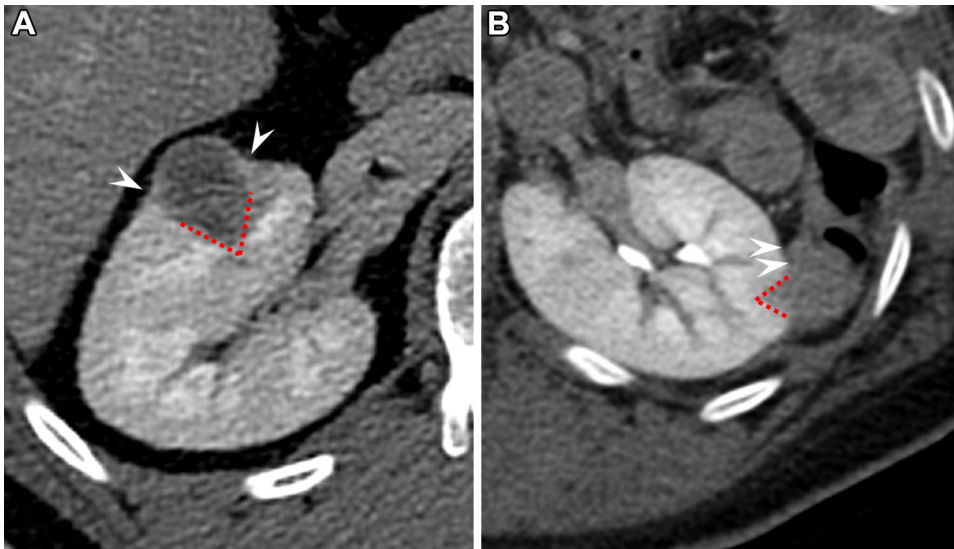


Fig. 3. **A** CT image of a 32-year-old man depicts a mass, measuring 2.5 cm, in the right kidney. The angular interface is seen (dotted red line), whereas overflowing beer sign is absent (arrowheads) for the lesion. The RCC was confirmed surgically. **B** CT image of a 49-year-old woman depicts a mass without gross fat, measuring 2.3 cm, in the left kidney. Both angular interface (dotted red line) and overflowing beer sign (arrowheads) are seen for the lesion. AML was confirmed surgically.

ROC curve analysis

The contact length between bulging-out portion of a mass and the adjacent renal surface was significantly longer in fpAML than in RCC (mean \pm standard deviation, 3.3 ± 2.7 mm versus 0.1 ± 0.8 mm; $p < 0.001$). The proportion of an angle within the parenchymal portion was also significantly different between fpAML and RCC (rate of angle $\leq 90^\circ$, 55.1% in fpAML versus 18.1% in RCC; $p < 0.001$).

In ROC curve analysis, the AUC of overflowing beer sign and angular interface were 0.795 (95% confidence interval [CI] 0.761–0.827) and 0.686 (95% CI 0.648–0.723) ($p = 0.019$). The optimal cutoff of morphologic parameters indicating fpAML was 3 mm or greater for overflowing beer sign and 90° or less for angular interface.

When the presence of both CT parameters is considered as a positive sign for fpAML, the AUC was 0.687. This was significantly lower than the AUC of overflowing beer sign ($p = 0.001$).

Diagnostic performance of overflowing beer sign and angular interface

Using the optimal cutoff of CT parameters derived from ROC curve analysis, the sensitivity, specificity, PPV,

NPV, and accuracy for diagnosing fpAML were 61.2% (30/49), 97.1% (537/553), 65.2% (30/46), 96.6% (537/556), and 94.2% (567/602) with overflowing beer sign, while those were 55.1% (27/49), 81.9% (453/553), 21.3% (27/127), 95.4% (453/475), and 79.7% (480/602) with angular interface, respectively (Table 2).

The specificity, PPV, and accuracy of overflowing beer sign were significantly higher than those of angular interface ($p < 0.001$) (Fig. 3 and 4). However, the sensitivity and NPV were similar between the two CT parameters ($p > 0.05$).

In addition, the PPV was 70.4% (19/27) when the two CT parameters are present, and NPV was 97.6% (445/456) when the two CT parameters are absent.

Estimated predictive values of overflowing beer sign and angular interface

On the basis of the previous studies with large population, the prevalence of AML ranged from 4.4% to 12.6% in patients with small renal masses [3–6]. The estimated PPV of overflowing beer sign was generally higher than that of angular interface (Table 3), while the estimated NPV was similarly excellent for predicting fpAML (Fig. 5).

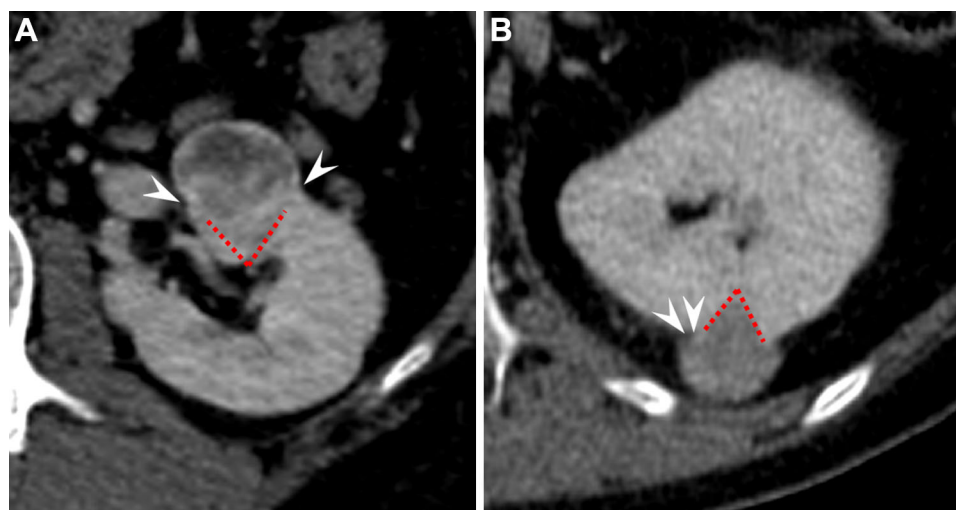


Fig. 4. **A** CT image of a 30-year-old woman depicts a mass, measuring 2.5 cm, in the left kidney. The angular interface is seen (dotted red line), whereas overflowing beer sign is absent (arrowheads) for the lesion. The RCC was confirmed surgically.

B CT image of a 39-year-old woman depicts a mass without gross fat, measuring 2.0 cm, in the left kidney. Both angular interface (dotted red line) and overflowing beer sign (arrowheads) are seen for the lesion. AML was confirmed surgically.

Table 3. Estimated predictive values of overflowing beer sign and angular interface for diagnosing fpAML

Reference	Prevalence	Positive predictive value		Negative predictive value	
		Overflowing beer sign	Angular interface	Overflowing beer sign	Angular interface
Pahernik et al. [3]	4.4 (25/578)	49.3 (31.5–67.3)	12.3 (7.0–19.6)	98.2 (96.7–99.1)	97.5 (95.7–98.7)
Richard et al. [4]	9.2 (36/391)	68.2 (53.5–80.7)	23.6 (16.6–31.9)	96.1 (94.1–97.6)	94.7 (92.3–96.6)
Remzi et al. [5]	5.0 (12/239)	52.7 (35.2–69.8)	13.8 (8.2–21.3)	97.9 (96.4–98.9)	97.2 (95.3–98.5)
Sasiwimonphan et al. [6]	12.6 (15/104)	75.3 (62.7–85.4)	30.5 (22.9–39.0)	94.6 (93.0–96.3)	92.7 (89.9–94.9)
Our own data	8.1 (49/602)	65.2 (49.8–78.7)	21.3 (14.5–29.4)	96.6 (94.7–97.9)	95.4 (93.1–97.1)

Estimated PPV and NPV of CT parameters were calculated based on Bayes' theorem using the prevalence of published studies [23]

The data of prevalence are % (number of patients)

The data of PPV and NPV are % (95% confidence interval)

Univariate and multivariate analyses

In univariate analysis, younger age (odds ratio [OR] 0.974, $p = 0.018$), female sex (OR 0.108, $p < 0.001$), smaller tumor size (OR 0.429, $p < 0.001$), and positive overflowing beer sign (OR 52.991, $p < 0.001$) or angular interface (OR 5.560, $p < 0.001$) were significantly associated with fpAML.

In the multivariate analysis, the overflowing beer sign or angular interface was predictive of fpAML (overflowing beer sign, OR 132.881, $p < 0.001$; angular interface, OR 5.766, $p < 0.001$) (Table 4). In addition, the diagnostic performance of models 1 to 4 by representing AUC was 0.824, 0.871, 0.943, and 0.949. The AUC of model 2, 3, or 4 with the morphologic analysis was significantly higher than that of model 1 (model 1 versus 2, $p = 0.038$; model 1 versus 3, $p < 0.001$; model 1 versus 4, $p < 0.001$). The AUC of model 3 or 4 including overflowing beer sign with/without angular interface was significantly higher than that of model 2 including angular interface ($p < 0.001$ in either com-

parison). However, there was no significant difference between models 3 and 4 ($p = 0.675$).

Discussion

In this study, both angular interface (OR 5.766, $p < 0.001$; c-index = 0.871 for a model with angular interface) and overflowing beer sign (OR 132.881, $p < 0.001$; c-index = 0.943 for a model with overflowing beer sign) were independent imaging parameters in differentiating fpAML from RCC. However, a prediction model with overflowing beer sign may have better discriminatory ability than a model with angular interface sign on contrast-enhanced CT ($p < 0.001$). In addition, from the data of multivariate logistic regression such as model 4, we can assume that conditions of younger age, female gender, smaller tumor size, and positive overflowing beer sign with/without angular interface raise the likelihood of fpAML.

Reportedly, the prevalence of RCC is much higher than that of fpAML in patients with a small renal mass

[3–6]. Therefore, we analyzed the predictive values of CT parameters using large, consecutive population with fpAML or RCC because PPV or NPV can be affected by the disease prevalence. In this study, PPV of angular interface (21.3%) was significantly lower than that of overflowing beer sign (65.2%) although a small proportion of patients with RCC had positive angular interface (18.1%, 100/553). The unbalanced incidence rate between fpAML and RCC might be related to the current results. However, NPVs of the two CT parameters were similarly excellent for fpAML (more than 95%). In addition, NPV was 97.6% (445/456) when the two CT parameters are negative. This indicates that concurrent absence of both angular interface and overflowing beer sign (e.g., round



Fig. 5. CT image of a 52-year-old woman depicts a mass, measuring 2.9 cm, in the right kidney. No angular interface (*dotted red line*) or overflowing beer sign (*arrowheads*) is seen for the lesion. RCC was confirmed surgically.

shape) on contrast-enhanced CT is suggestive of RCC more likely than fpAML.

We also calculated the estimated predictive values of CT parameters on the basis of previously reported data in terms of the prevalence of RCC and fpAML. The proportion of fpAML in this study was 8.1% (49/602), which is in line with previous reports (4%–13%). All the estimated predictive values showed concordant patterns of PPV and NPV between overflowing beer sign and angular interface: (a) higher estimated PPV of overflowing beer sign than angular interface; (b) similar and excellent estimated NPV between overflowing beer sign and angular interface. Overflowing beer sign seems to be a more specific imaging biomarker for fpAML, which may help plan the diagnostic or therapeutic strategies by reducing unnecessary biopsy or surgery.

RCC typically exhibits a slow, expansile growth with compact tumor cells and peripheral pseudocapsule in small size [26–28]. On the contrary, AML seems to be softer in tissue characteristics than RCC [29, 30] and often has no capsule or pseudocapsule at the periphery [19]. A recent pathologic study reported that smooth muscle-predominated AMLs are found in the subcapsular and cortical parenchyma, while fat-predominated AMLs are found in the medulla and corticomedullary junction [31]. These findings suggest that the growth pattern of AML can be affected more by adjacent structures, which may explain the morphologic features of small fpAML seen in this study: (a) narrow, angular configuration within the renal parenchyma (e.g., angular interface) and (b) a certain degree of free extension of bulging-out portion along the renal surface (e.g., overflowing beer sign).

There are several limitations in this study. First, various solid renal lesions such as the oncocytoma were not included in this study. The oncocytoma also manifests as a round, solid renal mass in small size on CT [32]. However, if some benign tumors show overflowing beer sign or angular interface mimicking AML, they would be considered as benign lesions although they are not true

Table 4. Multivariate analysis

Parameter	Multivariate model 1		Multivariate model 2		Multivariate model 3		Multivariate model 4	
	Odds ratio	<i>p</i> value	Odds ratio	<i>p</i> value	Odds ratio	<i>p</i> value	Odds ratio	<i>p</i> value
Age	0.967 (0.943–0.992)	0.001	0.974 (0.949–1.000)	0.049	0.943 (0.910–0.977)	0.049	0.946 (0.912–0.981)	0.003
Sex	0.099 (0.046–0.213)	<0.001	0.090 (0.041–0.199)	<0.001	0.089 (0.034–0.237)	<0.001	0.087 (0.032–0.233)	<0.001
Size	0.390 (0.240–0.632)	<0.001	0.399 (0.241–0.661)	<0.001	0.215 (0.108–0.428)	<0.001	0.221 (0.110–0.443)	<0.001
Angular interface			5.766 (2.926–11.364)	<0.001			2.514 (1.040–6.079)	0.040
Overflowing beer sign					132.881 (40.444–436.584)	<0.001	95.432 (28.570–318.772)	<0.001
P value*	0.656		0.313		0.641		0.885	
AUC**	0.824 (0.764–0.883)		0.871 (0.825–0.918)		0.943 (0.912–0.973)		0.949 (0.928–0.965)	

The data within parentheses are 95% confidence interval

* *p* value of Hosmer–Lemeshow goodness-of-fit test

** Area under the curve of multivariate models

AMLs. If they do not, then further radiologic investigations such as multiphasic CT, MRI, or biopsy could play a role in the characterization of the indeterminate lesions. Second, CT images were not obtained with a uniform protocol except the section thickness. Various CT scanners, tube current or voltage, and contrast agents were applied. This might be because our study was conducted in the tertiary institution. Conversely, our data may indicate the robustness of morphologic analysis, which may be widely applicable by using CT images of thin section. Third, the inter-reader agreement was not assessed. To minimize possible variability of the image interpretation, we only included the patients who underwent CT image with thin section (e.g., 3 mm). In addition, for the determination of overflowing beer sign, the contact length less than the section thickness of CT (e.g., less than 3 mm) was considered as the partial volume artifact. The angular interface was also determined quantitatively (e.g., angle of 90° or less). Accordingly, the process of image interpretation was relatively simple and straightforward. Fourth, only the CT images of section thickness of 3 mm or less were investigated. To evaluate whether the CT findings are feasible at thicker section (e.g., 5 mm), further validation studies are necessary with various CT protocols.

Conclusion

Morphologic analysis with contrast-enhanced CT may be useful for differentiation between fpAML and RCC. In addition, the overflowing beer sign has the potential to be used as an imaging biomarker predictive of fpAML.

Acknowledgments This research was supported by TAEJOON PHARM Co. Ltd., South Korea. There is no relevant financial conflict of interest. The authors would like to thank Dong-Su Jang, MFA, (Medical Illustrator, Medical Research Support Section, Yonsei University College of Medicine, Seoul, Korea) for his help with the illustrations.

Compliance with ethical standards

Conflict of interest None.

Ethical approval and Informed consent All procedures performed in studies involving human participants were in accordance with the ethical standards of the institutional research committee and with the 1964 Helsinki declaration and its later amendments or comparable ethical standards. Institutional review board at our institution approved this retrospective case-control study, and the requirement for informed consent was waived.

References

- Ljungberg B, Bensalah K, Canfield S, et al. (2015) EAU guidelines on renal cell carcinoma: 2014 update. *Eur Urol* 67(5):913–924
- Hindman N, Ngo L, Genega EM, et al. (2012) Angiomyolipoma with minimal fat: can it be differentiated from clear cell renal cell carcinoma by using standard MR techniques? *Radiology* 265(2):468–477
- Pahernik S, Ziegler S, Roos F, et al. (2007) Small renal tumors: correlation of clinical and pathological features with tumor size. *J Urol* 178(2):414–417 (discussion 416–417)
- Richard PO, Jewett MA, Bhatt JR, et al. (2015) Renal tumor biopsy for small renal masses: a single-center 13-year experience. *Eur Urol* 68(6):1007–1013
- Remzi M, Ozsoy M, Klingler HC, et al. (2006) Are small renal tumors harmless? Analysis of histopathological features according to tumors 4 cm or less in diameter. *J Urol* 176(3):896–899
- Sasiwimonphan K, Takahashi N, Leibovich BC, et al. (2012) Small (<4 cm) renal mass: differentiation of angiomyolipoma without visible fat from renal cell carcinoma utilizing MR imaging. *Radiology* 263(1):160–168
- Patel HD, Johnson MH, Pierorazio PM, et al. (2016) Diagnostic accuracy and risks of biopsy in the diagnosis of a renal mass suspicious for localized renal cell carcinoma: systematic review of the literature. *J Urol* 195(5):1340–1347
- Marconi L, Dabestani S, Lam TB, et al. (2016) Systematic review and meta-analysis of diagnostic accuracy of percutaneous renal tumour biopsy. *Eur Urol* 69(4):660–673
- Sharma KV, Venkatesan AM, Swerdlow D, et al. (2010) Image-guided adrenal and renal biopsy. *Tech Vasc Interv Radiol* 13(2):100–109
- Leveridge MJ, Finelli A, Kachura JR, et al. (2011) Outcomes of small renal mass needle core biopsy, nondiagnostic percutaneous biopsy, and the role of repeat biopsy. *Eur Urol* 60(3):578–584
- Jeon HG, Seo SI, Jeong BC, et al. (2016) Percutaneous kidney biopsy for a small renal mass: a critical appraisal of results. *J Urol* 195(3):568–573
- Kim JK, Park SY, Shon JH, et al. (2004) Angiomyolipoma with minimal fat: differentiation from renal cell carcinoma at biphasic helical CT. *Radiology* 230(3):677–684
- Schieda N, Hodgdon T, El-Khodary M, et al. (2014) Unenhanced CT for the diagnosis of minimal-fat renal angiomyolipoma. *AJR Am J Roentgenol* 203(6):1236–1241
- Kim JY, Kim JK, Kim N, et al. (2008) CT histogram analysis: differentiation of angiomyolipoma without visible fat from renal cell carcinoma at CT imaging. *Radiology* 246(2):472–479
- Birnbaum BA, Hindman N, Lee J, et al. (2007) Multi-detector row CT attenuation measurements: assessment of intra- and interscanner variability with an anthropomorphic body CT phantom. *Radiology* 242(1):109–119
- Bae KT (2010) Intravenous contrast medium administration and scan timing at CT: considerations and approaches. *Radiology* 256(1):32–61
- Verma SK, Mitchell DG, Yang R, et al. (2010) Exophytic renal masses: angular interface with renal parenchyma for distinguishing benign from malignant lesions at MR imaging. *Radiology* 255(2):501–507
- Yang CW, Shen SH, Chang YH, et al. (2013) Are there useful CT features to differentiate renal cell carcinoma from lipid-poor renal angiomyolipoma? *AJR Am J Roentgenol* 201(5):1017–1028
- Sung CK, Kim SH, Woo S, et al. (2016) Angiomyolipoma with minimal fat: differentiation of morphological and enhancement features from renal cell carcinoma at CT imaging. *Acta Radiol* 57(9):1114–1122
- Barrett JF, Keat N (2004) Artifacts in CT: recognition and avoidance. *Radiographics* 24(6):1679–1691
- Silverman SG, Israel GM, Herts BR, et al. (2008) Management of the incidental renal mass. *Radiology* 249(1):16–31
- Jinzaki M, Silverman SG, Akita H, et al. (2014) Renal angiomyolipoma: a radiological classification and update on recent developments in diagnosis and management. *Abdom Imaging* 39(3):588–604
- Halpern EF, Gazelle GS (2003) Probability in radiology. *Radiology* 226(1):12–15
- Harrell FE Jr, Lee KL, Mark DB (1996) Multivariable prognostic models: issues in developing models, evaluating assumptions and adequacy, and measuring and reducing errors. *Stat Med* 15(4):361–387
- Han K, Song K, Choi BW (2016) How to develop, validate, and compare clinical prediction models involving radiological parameters: study design and statistical methods. *Korean J Radiol* 17(3):339–350
- Yamashita Y, Honda S, Nishiharu T, et al. (1996) Detection of pseudocapsule of renal cell carcinoma with MR imaging and CT. *AJR Am J Roentgenol* 166(5):1151–1155

27. Gurel S, Narra V, Elsayes KM, et al. (2013) Subtypes of renal cell carcinoma: MRI and pathological features. *Diagn Interv Radiol* 19(4):304–311
28. Diaz JI, Mora LB, Hakam A (1999) The Mainz classification of renal cell tumors. *Cancer Control* 6(6):571–579
29. Tan S, Ozcan MF, Tezcan F, et al. (2013) Real-time elastography for distinguishing angiomyolipoma from renal cell carcinoma: preliminary observations. *AJR Am J Roentgenol* 200(4):W369–W375
30. Onur MR, Poyraz AK, Bozgeyik Z, et al. (2015) Utility of semi-quantitative strain elastography for differentiation between benign and malignant solid renal masses. *J Ultrasound Med* 34(4):639–647
31. Calio A, Warfel KA, Eble JN (2016) Pathological features and clinical associations of 58 small incidental angiomyolipomas of the kidney. *Hum Pathol* 58:41–46
32. Dyer R, DiSantis DJ, McClennan BL (2008) Simplified imaging approach for evaluation of the solid renal mass in adults. *Radiology* 247(2):331–343